

# NUMERICAL AVERAGING OF NON-DIVERGENCE STRUCTURE ELLIPTIC OPERATORS

BRITTANY D. FROESE AND ADAM M. OBERMAN

ABSTRACT. Many important equations in science and engineering contain rapidly varying operators that cannot practically be resolved sufficiently for accurate solutions. In some cases it is possible to obtain approximate solutions by replacing the rapidly varying operator with an appropriately averaged operator. In this paper we use formal asymptotic techniques to recover a formula for the averaged form of a second order, non-divergence structure, linear elliptic operator. For several special cases the averaged operator is obtained analytically. For genuinely multi-dimensional cases, the averaged operator is also obtained numerically, using a finite difference method, which also has a probabilistic interpretation.

## CONTENTS

1. Introduction	2
1.1. Contents	2
1.2. Goals of this Paper	2
1.3. Related Work	3
2. The Averaging Formula	3
2.1. The Fredholm Alternative and the Invariant Distribution	4
2.2. The Averaged Coefficients	5
3. Explicit Solutions	6
3.1. Multiples of a Constant Coefficient Matrix	7
3.2. A Special Case: Layered Material	8
3.3. A Special Case: Separable, Diagonal Coefficient Matrix	8
4. Comparison with Divergence Structure Results	10
4.1. A Layered Material	10
4.2. A Separable Material	10
5. Numerical Results	11
5.1. Discretisation and Numerical Solution	11
5.2. Multiples of a Constant Coefficient Matrix	12
5.3. A Layered Material	14
5.4. A Separable, Diagonal Coefficient Matrix	15
5.5. A More General Linear Operator	16
5.6. Non-Zero Boundary Conditions	17
5.7. Random Coefficients	19
6. Conclusions	22
References	23

---

*Date:* May 18, 2009.

## 1. INTRODUCTION

Second order elliptic equations—in both divergence and non-divergence form—arise frequently in areas such as science and engineering [6]. When the operators involved vary rapidly on a small spatial scale these problems carry an additional challenge since it is generally not practical to resolve the computational domain enough to capture the behaviour of the operator. A resolution to this challenge is replacing the original operator with a different, slowly varying operator with solutions that are close to the solutions of the original problem. In this divergence structure case the problem is of homogenization, and the solution is provided by the cell problem. In the nondivergence structure case studied herein, the macroscopic coefficients are simply averages of the original terms against the invariant measure, and the problem is called averaging. (There is some inconsistency in the literature concerning terminology, we follow [8].)

**1.1. Contents.** The first section of this paper is introductory. Section two gives the theoretical basis for the averaging formula. Section three provides explicit analytical solutions. Section four gives a comparison with known analytical results in the divergence structure case, when these are available. Section five is numerical, it begins with a discussion of the discretization and follows with numerical computations. The final section gives the conclusions.

**1.2. Goals of this Paper.** Let  $L^\epsilon$  denote the following non-degenerate elliptic differential operator

$$(1.1) \quad L^\epsilon = - \sum_{i,j=1}^n a_{ij}(x/\epsilon) \frac{\partial^2}{\partial x_i \partial x_j} + \sum_{i=1}^n b_i(x/\epsilon) \frac{\partial}{\partial x_i} + c(x/\epsilon)$$

Here we assume that the coefficients  $A = (a)_{ij}$ ,  $b = (b)_i$ , and  $c$  are periodic of period one in all their arguments and belong to  $C^1(\mathbb{R}^n)$ . We study the problem

$$(PDE)^\epsilon \quad \begin{cases} L^\epsilon u^\epsilon = f(x), & \text{for } x \in U \\ u^\epsilon = g(x), & \text{for } x \in \partial U \end{cases}$$

in a bounded domain  $U \subset \mathbb{R}^n$  with smooth boundary  $\partial U$ . Here for simplicity,  $f(x)$ ,  $g(x)$  are continuous functions on  $U$ ,  $\partial U$ , respectively.

Our goal is approximation of  $(PDE)^\epsilon$  for small  $\epsilon$  using a homogeneous operator on a coarsely resolved finite difference grid. This goal is accomplished by recovering, using both analytical and numerical techniques, the averaged operator which is the limit of the operators  $L^\epsilon$  as  $\epsilon \rightarrow 0$ .

In the first part of this paper we use formal asymptotic calculations to recover an analytic formula for the averaged operator (first obtained by Freidlin [3] using probabilistic methods). The averaged operator is given in terms of the invariant distribution for the dynamics, which is the solution of a PDE involving the adjoint operator. In several special cases we obtain explicit representations of the invariant distribution so that the averaged operator can be expressed in closed form. These special cases require additional structure on the coefficients.

In the general, genuinely multidimensional case, there is no analytical formula for the invariant distribution available. However, the the PDE for the invariant

distribution can be solved numerically on a relatively coarse grid. Numerical examples are computed, the method is validated by recovering the known solutions, and new examples are computed.

**1.3. Related Work.** Homogenisation (and averaging to a lesser extent) have received much attention in recent years; see the books [4, 8, 1] and the survey [2]. We are grateful to the authors of [8], which influenced our approach.

Early work by Freidlin [3] used probabilistic methods to average the inhomogeneous, non divergence-structure equation  $(\text{PDE})^\epsilon$ . The non-divergence equation has a probabilistic interpretation. Freidlin averaged the operator by considering the limiting distribution of the underlying stochastic differential equation. The operator is the generator for the diffusion and arises as the backward Kolmogorov equation. The evolution of densities satisfies the Fokker-Planck equation, which involves the adjoint operator, see also [8, Chapter 6].

There is considerably more work on divergence structure equations, either in the variational form

$$(1.2) \quad -\nabla \cdot (A(x/\epsilon)\nabla u) = f$$

or expanded into the singular form (see notation in the next section)

$$(1.3) \quad -A(x/\epsilon) : D^2u + \frac{1}{\epsilon}b(x/\epsilon) \cdot \nabla u = f.$$

While the problems  $(\text{PDE})^\epsilon$  and (1.3) are equivalent for fixed  $\epsilon$ , provided the coefficients are smooth enough, we note that the non-divergence structure equation  $(\text{PDE})^\epsilon$  and the expanded divergence structure equation (1.3) are different in the limit  $\epsilon \rightarrow 0$ . This difference is due to the coefficient  $\epsilon^{-1}$  of the drift term  $b$  in the divergence structure problem. References to works in the divergence structure setting can be found in the textbooks mentioned above. We draw the attention of the reader to the recent work [7].

In very simple cases, both the divergence structure and non-divergence structure operators average (homogenise) to the harmonic mean. However, in general the results are different. For example, in the simple case of separable operators, where analytical results are available, the results are different; see Section §3.3.

## 2. THE AVERAGING FORMULA

In this section we use formal asymptotic calculations and PDE methods to average the operator (1.1). This section uses an argument similar to Part II of [8], which gave the homogenisation formula for divergence structure elliptic equations. The formal calculations can be made rigorous, following the method of Part III of [8].

Use the notation

$$(D^2)_{ij} = \frac{\partial^2}{\partial x_i \partial x_j}, \quad \nabla = (\partial x_1, \dots, \partial x_n)$$

for the Hessian operator and the gradient operator, respectively. Use

$$M : N = \text{tr}(M^T N) = \sum_{i,j=1}^n M_{ij} N_{ij}$$

for the inner product between matrices and  $b \cdot d = \sum_{i=1}^n b_i d_i$  for the dot product of vectors. Rewrite  $L^\epsilon$  defined in (1.1) as

$$L^\epsilon = -A(x/\epsilon) : D^2 + b(x/\epsilon) \cdot \nabla + c(x/\epsilon)$$

Use angle brackets to denote the average over one periodic domain  $\Omega = [0, 1]^n$ ,

$$\langle v \rangle = \frac{\int_{\Omega} v}{|\Omega|}$$

**2.1. The Fredholm Alternative and the Invariant Distribution.** For completeness, we recall the Fredholm Alternative. Consider the operator

$$L_0(x) = -A(x) : D^2$$

where the coefficient matrix,  $A(x)$ , is periodic,  $C^1$ , and uniformly positive definite. The adjoint operator, which is also periodic, acts on a function  $v(x) \in C^2(\Omega)$  by

$$L_0^*(x)v(x) = -D^2 : (A(x)v(x)).$$

**Theorem 1** (The Fredholm Alternative [8]). *Consider the operator  $L_0(x) = -A(x) : D^2$ , where the coefficient matrix is periodic,  $C^1$ , and uniformly positive definite. Exactly one of the following conditions holds.*

- (1) *The equation  $L_0 u = f$  has a unique periodic solution for every  $f \in L^2_{per}(\Omega)$ .*
- (2) *The homogeneous equation  $L_0 u = 0$  has a non-trivial periodic solution, the nullspaces of  $L_0$  and its adjoint  $L_0^*$  have the same dimension, and the inhomogeneous equation  $L_0 u = f$  is solvable if and only if*

$$\langle f v \rangle = 0 \quad \text{for all } v \text{ in the kernel of } L_0^*.$$

Since the kernel of the operator  $L_0$  is one-dimensional (consisting only of constants), the kernel of the adjoint  $L_0^*$  is also one-dimensional, by the Fredholm Alternative. Thus the *invariant distribution*,  $\rho^\infty$ , is uniquely prescribed as the unique element of the kernel of the adjoint operator  $L_0^*$  [8, Theorem 6.16]

$$(2.1) \quad L_0^* \rho^\infty = -D^2 : (A \rho^\infty) = 0, \quad \text{in } \Omega$$

which satisfies the normalisation condition

$$(2.2) \quad \langle \rho^\infty \rangle = 1, \quad \rho^\infty \text{ is periodic in } y.$$

This leads to the following solvability condition.

**Theorem 2** (Solvability Condition). *Consider the operator  $L_0(x) = -A(x) : D^2$ , where the coefficient matrix is periodic,  $C^1$ , and uniformly positive definite. The equation*

$$L_0 u = f, \quad u \text{ is periodic}$$

*has a solution if and only if  $f$  is orthogonal to the nullspace of the adjoint operator, which can be verified by*

$$\langle \rho^\infty f \rangle = 0$$

*where  $\rho^\infty$  is the invariant distribution.*

## 2.2. The Averaged Coefficients.

**Theorem 3.** *Let the operator  $L^\epsilon$  be as in (1.1). Let  $\rho^\infty$  be the invariant distribution, given by the unique solution of (2.1), (2.2). Formally, in the limit  $\epsilon \rightarrow 0$ , solutions of the equation  $(PDE)^\epsilon$  converge to solutions of the averaged equation*

$$(PDE) \quad \begin{cases} \bar{L}u = f(x), & \text{for } x \in U \\ u = g(x) & \text{for } x \in \partial U \end{cases}$$

where

$$\bar{L} = -\bar{A} : D^2 + \bar{b} \cdot \nabla + \bar{c}$$

has coefficients given by averaging the original coefficients against the invariant distribution

$$(2.3) \quad \bar{A} = \langle \rho^\infty A \rangle, \quad \bar{b} = \langle \rho^\infty b \rangle, \quad \bar{c} = \langle \rho^\infty c \rangle.$$

In addition, formally,

$$(2.4) \quad u^\epsilon(x) = u_0(x) + O(\epsilon^2).$$

*Proof.* We begin the analysis by introducing a new variable

$$y = x/\epsilon$$

where  $\epsilon$  is the size of the small cells on which the coefficients vary. We assume the two scales  $x$  and  $y$  are independent and write the coefficients as

$$A(x/\epsilon) = A(y), \quad b(x/\epsilon) = b(y), \quad c(x/\epsilon) = c(y).$$

Since we are treating the two spatial scales as independent, rewrite the partial derivative  $\partial_{x_i}$  as

$$\partial_{x_i} + \frac{1}{\epsilon} \partial_{y_i}$$

The equation  $(PDE)^\epsilon$  then becomes

$$(2.5) \quad -\frac{1}{\epsilon^2} A : D_y^2 u^\epsilon + \frac{1}{\epsilon} (-2A : \nabla_x \nabla_y^T u^\epsilon + b \cdot \nabla_y u^\epsilon) + (-A : D_x^2 u^\epsilon + b \cdot \nabla_x u^\epsilon + c u^\epsilon) = f$$

Now we look for a solution of the form (we skip the step which shows odd order terms in  $\epsilon$  are not needed)

$$(2.6) \quad \begin{aligned} u^\epsilon(x) &= u_0(x, x/\epsilon) + \epsilon^2 u_2(x, x/\epsilon) + \dots \\ &= u_0(x, y) + \epsilon^2 u_2(x, y) + \dots \end{aligned}$$

Substituting this solution form into the PDE (2.5) we obtain

$$(2.7) \quad \frac{1}{\epsilon^2} L_0 u_0 + \frac{1}{\epsilon} L_1 u_0 + (L_0 u_2 + L_2 u_0) + O(\epsilon) = f.$$

Here we have defined the operators

$$\begin{aligned} L_0 &= -A : D_y^2 \\ L_1 &= -2A : \nabla_x \nabla_y^T + b \cdot \nabla_y \\ L_2 &= -A : D_x^2 + b \cdot \nabla_x + c \end{aligned}$$

To ensure that  $u^\epsilon$  satisfies the required boundary conditions we also enforce the appropriate boundary conditions on the terms in the asymptotic expansion (2.6). For the leading order term we require

$$\begin{cases} u_0 = g(x) & \text{on } \partial U \\ u_0 & \text{periodic in } y \end{cases}$$

For  $k > 0$  we enforce

$$\begin{cases} u_k = 0 & \text{on } \partial U \\ u_k & \text{periodic in } y \end{cases}$$

We first look at the leading order,  $O(\frac{1}{\epsilon^2})$ , terms in (2.7) to obtain the equation

$$\begin{cases} -A : D_y^2 u_0 = 0 \\ u_0 \text{ is periodic in the } y \text{ variable} \end{cases}$$

Because of the periodic boundary conditions (in  $y$ ), the solution of this equation will be independent of the  $y$  variable:

$$u_0 = u_0(x)$$

Next we consider the  $O(\frac{1}{\epsilon})$  terms in (2.7) to obtain

$$-2A : \nabla_x \nabla_y^T u_0 + b \cdot \nabla_y u_0 = 0$$

This is automatically satisfied since  $u_0$  is independent of  $y$ .

Finally, we consider the  $O(1)$  terms in (2.7) to obtain the equation

$$(2.8) \quad -A : D_y^2 u_2 = A : D_x^2 u_0 - b \cdot \nabla_x u_0 - c u_0 + f.$$

We can now use the Theorem 2 to obtain a solvability condition for (2.8):

$$\int_{\Omega} \rho^\infty (A : D_x^2 u_0 - b \cdot \nabla_x u_0 - c u_0 + f) dy = 0$$

Because  $u_0$  and  $f$  are independent of the  $y$  variable and the solution of the adjoint problem is normalised we can integrate the last equation to obtain

$$(2.9) \quad -\bar{A} : D_x^2 u_0 + \bar{b} \cdot \nabla_x u_0 + \bar{c} u_0 = f$$

where the averaged coefficients are given by (2.3)

$$\bar{A} = \langle \rho^\infty A \rangle, \quad \bar{b} = \langle \rho^\infty b \rangle, \quad \bar{c} = \langle \rho^\infty c \rangle.$$

Returning now to the asymptotic expansion for  $u^\epsilon$  (2.6), we see that (2.4) holds, where  $u_0$  satisfies the averaged equation (2.9).  $\square$

### 3. EXPLICIT SOLUTIONS

In this section we consider a number of special cases for which we can solve the adjoint problem (2.1) exactly. In these cases we can generate explicit formulas for the averaged operators.

We provide a visual representation of several of these operators by plotting the ellipses given by the equation  $y^T A y = 1$ . The shading of these pictures is such that lighter colouring corresponds to larger entries in the coefficient matrix.

*Remark.* Since the lower order terms average in the same way as the coefficient matrix, but do not affect the formula for the invariant distribution, we omit them to shorten the exposition.

**3.1. Multiples of a Constant Coefficient Matrix.** One of the simplest cases involves a coefficient matrix that is a (variable) scalar multiple of a constant matrix

$$A(x/\epsilon) = a(x/\epsilon)B,$$

which yields the harmonic mean

$$(3.1) \quad \bar{A} = \langle a(y)^{-1} \rangle^{-1} B.$$

A typical example is illustrated in Figure 1, which is the piecewise constant periodic checkerboard.

As a special case we recover the well-known one-dimensional result which follows. The operator

$$-a(x/\epsilon)u_{xx} = f$$

homogenises to the harmonic mean

$$(3.2) \quad \bar{a} = \langle a(y)^{-1} \rangle^{-1}.$$

*Calculation.* The adjoint problem (2.1) becomes

$$-B : D_y^2(a(y)\rho^\infty(y)) = 0$$

with solution  $\rho^\infty(y) = a(y)^{-1} \langle a(y)^{-1} \rangle^{-1}$  yielding (3.1). In particular (since  $B$  is constant) we see that each element in the coefficient matrix homogenises to its harmonic mean:

$$(3.3) \quad \bar{a}_{i,j} = \langle a(y)^{-1} b_{ij}^{-1} \rangle^{-1} = \langle a_{ij}(y)^{-1} \rangle^{-1}. \quad \square$$

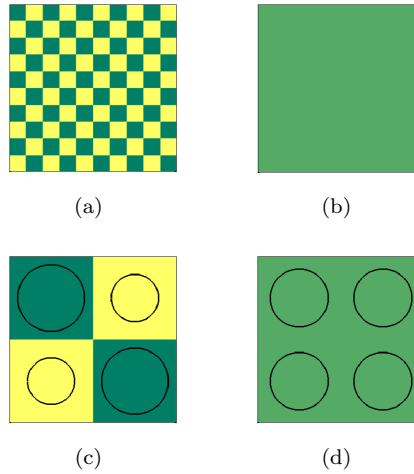


FIGURE 1. A visual representation of a piecewise constant multiple of the Laplacian on a periodic checkerboard. (a) The original grid. (b) The homogenised grid. (c) The original operator on one small cell. (d) The homogenised operator on one small cell.

**3.2. A Special Case: Layered Material.** Next we consider the special case of a layered material, where the coefficient matrix is a function of only one variable:

$$A(y) = A(y_1)$$

See Figure 2 for a visualisation of the operator.

The adjoint equation is now

$$-D_y^2(A(y_1)\rho^\infty(y)) = 0,$$

which has the solution

$$\rho^\infty(y) = a_{11}(y_1)^{-1} \langle a_{11}(y_1)^{-1} \rangle^{-1}.$$

Thus the averaged coefficient matrix from (2.3) is

$$(3.4) \quad \bar{A} = \langle a_{11}^{-1} \rangle^{-1} \langle a_{11}^{-1} A \rangle.$$

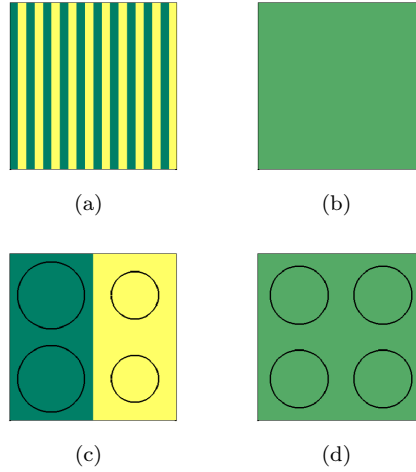


FIGURE 2. A visual representation of a piecewise constant multiple of the Laplacian on a layered material. (a) The original grid. (b) The homogenised grid. (c) The original operator on one small cell. (d) The homogenised operator on one small cell.

**3.3. A Special Case: Separable, Diagonal Coefficient Matrix.** We also consider the case where the coefficient matrix is diagonal and has separable entries. That is, the matrix can be expressed as a product of diagonal matrices of the form

$$A(y) = \prod_{j=1}^n A^j(y_j)$$

and each entry on the diagonal of the resulting matrix can be written as

$$A_{ii}(y) = \prod_{i=1}^n A_{ii}^j(y_j).$$

See Figure 3 for a visualisation of such an operator. The averaged coefficients are

$$(3.5) \quad \bar{A} = \left\langle \frac{1}{\prod_{j=1}^n A_{jj}^j(y_j)} A \right\rangle \left\langle \frac{1}{\prod_{j=1}^n A_{jj}^j(y_j)} \right\rangle^{-1}$$

as can be verified by the calculation which follows.

*Calculation.* In this case, the adjoint equation (2.1) takes the form

$$-\sum_{i=1}^n \left( \prod_{j=1}^n A_{ii}^j(y_j) \rho^\infty(y) \right)_{y_i y_i} = 0$$

Since the coefficients are separable, the invariant distribution will also be separable:

$$\rho^\infty = \frac{1}{\prod_{j=1}^n A_{jj}^j(y_j)} \left\langle \frac{1}{\prod_{j=1}^n A_{jj}^j(y_j)} \right\rangle^{-1}$$

and the result follows by averaging using (2.3). □

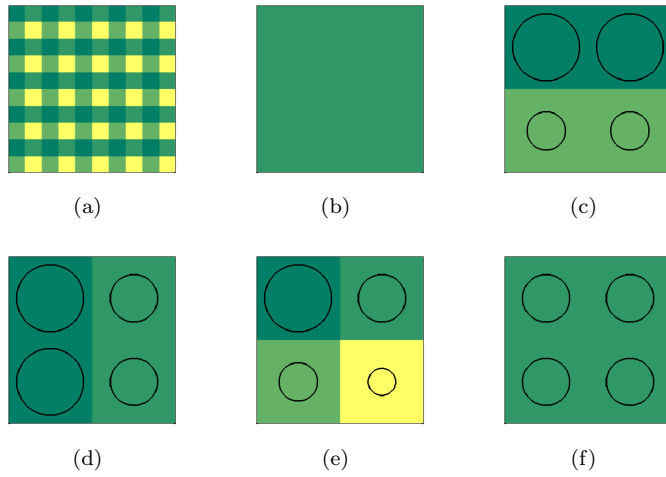


FIGURE 3. A visual representation of a separable operator. (a) The original grid. (b) The homogenised grid. (c) The vertical structure of the operator on one small cell. (d) The horizontal structure of the operator on one small cell. (e) The original operator on one small cell. (f) The averaged operator on one small cell.

## 4. COMPARISON WITH DIVERGENCE STRUCTURE RESULTS

A given coefficient matrix,  $A$ , can be used to generate either the non-divergence structure operator (1.1)

$$L^\epsilon u = -A(x/\epsilon) : D^2 u,$$

or the divergence structure operator (1.2)

$$L_{div}^\epsilon u = -\nabla \cdot (A(x/\epsilon) \nabla u).$$

Only in very simple cases will the coefficient matrix  $A$  homogenise to the same operator for both the divergence and non-divergence case. The main example where the results are the same is the one-dimensional case, where the coefficient matrix homogenises to the harmonic mean for both problems [8], (3.2). However, in general the two operators will result in different homogenised coefficients.

For the convenience of the reader we compare the explicit solutions of §3 to known results for the divergence structure problem.

**4.1. A Layered Material.** First we consider a two-dimensional layered material. The divergence structure result is given in [8]. Although most elements of the coefficient matrix average in the same way for both problems, one element is different. In the non-divergence structure case we obtain from (3.4)

$$\bar{a}_{22} = \langle a_{11}^{-1} \rangle^{-1} \left\langle \frac{a_{22}}{a_{11}} \right\rangle.$$

The divergence case, on the other hand, yields

$$\bar{a}_{22}^{div} = \left\langle \frac{a_{21}}{a_{11}} \right\rangle \left\langle \frac{a_{12}}{a_{11}} \right\rangle \langle a_{11}^{-1} \rangle^{-1} + \left\langle a_{22} - \frac{a_{12}a_{21}}{a_{11}} \right\rangle.$$

**4.2. A Separable Material.** We can also consider a two-dimensional separable operator that is a scalar multiple of the identity.

$$A(x/\epsilon) = a_1(x_1/\epsilon)a_2(x_2/\epsilon)I$$

This is a special case of both the constant operator of §3.1 and the separable case of §3.3. In either case, the coefficients for the non-divergence structure problem homogenises to the constant multiple of the identity, given by a generalised harmonic mean,

$$\bar{A} = \langle a_1^{-1} a_2^{-1} \rangle^{-1} I,$$

where  $I$  denotes the identity matrix. In the divergence problem, which is considered in [4], the homogenised coefficients are not all equal and are obtained from a combination of the harmonic and arithmetic means of the coefficients.

$$\begin{aligned} \bar{A}_{11}^{div} &= \langle a_2 \rangle \langle a_1^{-1} \rangle^{-1} \\ \bar{A}_{22}^{div} &= \langle a_1 \rangle \langle a_2^{-1} \rangle^{-1}. \end{aligned}$$

## 5. NUMERICAL RESULTS

Although there are a number of situations in which we can write down an explicit representation of the averaged coefficients, this is not always possible. However, the homogenisation result can be implemented numerically. To accomplish this we need only solve one linear equation, (2.1), along with the normalisation constraint (2.2). The computational effort is comparable (arguably less) to the effort for the divergence structure problem, where  $n$  equations must be solved for the cell problem.

The finite difference schemes we use have a natural interpretation as a discrete space Markov chain approximation of the underlying diffusion process. Consequently, one approach to interpreting the numerical method would be to use Markov chain approximations along the lines of [5, 10, 9]. Here we will focus on the PDE aspects in order to discretise the problem. To present the ideas in the simplest setting, we perform the discretisation in two dimensions; the generalisation to higher dimensions is accomplished by standard techniques.

In this section we numerically average several test problems and solve the averaged equations. We demonstrate that the approach presented in this paper does correctly average the non-divergence structure elliptic operator and compute the operators in some cases where the exact formula is not known. We begin by validating the approach: we demonstrate numerically that the solutions of the original equation

$$A(x/\epsilon) : D^2 u^\epsilon = f$$

converge pointwise to the solutions of the averaged equation

$$\bar{A} : D^2 u = f$$

in the limit as  $\epsilon \rightarrow 0$ .

A further goal of this section is to investigate the relationship between cell resolution and accuracy of both the computed averaged operators and the solutions of the averaged equations.

*Notation for this section.* Below we denote by  $\text{diag}(a)$  the diagonal matrix whose  $j^{\text{th}}$  diagonal element is given by the  $j^{\text{th}}$  element of the vector  $a$ . We use  $\mathbf{0}, \mathbf{1}$  for vectors whose elements are identically zero or one respectively. The identity matrix is represented by  $I$ .

**5.1. Discretisation and Numerical Solution.** We will be solving the non-divergence form equation  $(\text{PDE})^\epsilon$ . This is discretised using centred differences and the linear systems was solved directly (in this case using the default Matlab backslash solver). In all cases, the computational domain is the unit square  $[0, 1] \times [0, 1]$ .

We also want to solve Equation (2.1) for the invariant distribution. Let  $\rho = (\rho_{ij})$  be a grid vector indexed by the grid coefficients. The fact that the grid vector  $\rho$  approximates the solution  $\rho^\infty$  at the corresponding grid points,

$$\rho_{ij} = \rho^\infty(hi, hj) + O(h^2)$$

will follow from the standard linear finite difference analysis. After discretising the two-dimensional adjoint equation (2.1) by standard centered finite differences, with spatial resolution,  $h$ , we obtain a finite dimensional linear equation.

$$(5.1) \quad M\rho = 0,$$

where  $M$  is a linear operator defined below, along with the discretisation of the constraint (2.2)

$$(5.2) \quad \sum_{i,j} \rho_{ij} h^2 = 1.$$

The matrix  $M$  is obtained by combining the finite difference operators, for each term as follows. To shorten the formulas, write the grid matrix  $A = A_{ij}$  as a collection of scalar functions for each component

$$A = A_{ij} = \begin{pmatrix} a_{11} & a_{12} \\ a_{21} & a_{22} \end{pmatrix}_{ij} = \begin{pmatrix} q_{ij} & s_{ij} \\ s_{ij} & r_{ij} \end{pmatrix}.$$

Then define the linear operators

$$Q = \text{diag}(q_{ij}), \quad R = \text{diag}(r_{ij}), \quad S = \text{diag}(s_{ij})$$

which correspond to scalar multiplication. Next define  $D_{y_1 y_1}, D_{y_1 y_2}, D_{y_2 y_2}$  to be the linear operators corresponding to the finite difference operators for the second derivatives. The equation (5.1) then takes the form

$$(5.3) \quad (D_{y_1 y_1} Q + D_{y_2 y_2} R + 2D_{y_1 y_2} S) \rho = 0.$$

Writing out the operator more explicitly, term by term, results in

$$(5.4) \quad \begin{aligned} (D_{y_1 y_1} Q \rho)_{ij} &= \frac{1}{h^2} (q_{i+1,j} \rho_{i+1,j} + q_{i-1,j} \rho_{i-1,j} - 2q_{i,j} \rho_{i,j}) \\ (D_{y_2 y_2} R \rho)_{ij} &= \frac{1}{h^2} (r_{i,j+1} \rho_{i,j+1} + r_{i,j-1} \rho_{i,j-1} - 2r_{i,j} \rho_{i,j}) \\ 2(D_{y_1 y_2} S \rho)_{ij} &= \frac{2}{h^2} (s_{i+1,j+1} \rho_{i+1,j+1} + s_{i-1,j-1} \rho_{i-1,j-1} \\ &\quad - s_{i+1,j-1} \rho_{i+1,j-1} - s_{i-1,j+1} \rho_{i-1,j+1}) \end{aligned}$$

The equation (5.3) can be solved by a direct method, enforcing the single constraint (5.2). For simplicity, we solved the equation iteratively by a Gauss-Seidel method. Since the operator preserves mass, even at the discrete level, the constraint (5.2) was satisfied by choosing initial data which satisfied the constraint.

**5.2. Multiples of a Constant Coefficient Matrix.** We begin with a simple example, where the coefficient matrix is a (variable) scalar multiple of a constant matrix. That is

$$A = p(y)K$$

where  $K$  is a constant matrix.

We have already showed that the solution (3.1) of the adjoint equation is simply

$$\rho^\infty(y) = p(y)^{-1} \langle p(y)^{-1} \rangle^{-1}.$$

It is easy to see that this will also be a steady state solution of the discretised equation no matter what cell resolution we use. To demonstrate this, we make the following replacements in the discretised equation (5.4):

$$Q = k_{11}P, \quad R = k_{22}P, \quad S = k_{12}P.$$

Here  $P = \text{diag}(p)$  is a diagonal matrix and  $k_{11}, k_{22}, k_{12}$  are constant. The proposed steady state solution in discrete form is

$$\rho^\infty = P^{-1} \mathbf{1} \langle P^{-1} \mathbf{1} \rangle^{-1}.$$

Substituting these expressions into the discrete equation (5.4) we find that

$$\begin{aligned} D_{y_1 y_1} Q \rho^\infty &= D_{y_1 y_1} k_{11} P P^{-1} \mathbf{1} \langle P^{-1} \mathbf{1} \rangle^{-1} \\ &= k_{11} \langle P^{-1} \mathbf{1} \rangle^{-1} D_{y_1 y_1} \mathbf{1} \\ &= \mathbf{0} \end{aligned}$$

where the last step holds since the rows of  $D_{y_1 y_1}$  sum to one. The other terms vanish similarly, showing that (3.1) is in fact the steady state solution of the discrete iterative scheme (5.4) regardless of how well or poorly the cell is resolved.

We now choose a specific example where the coefficient matrix is piecewise constant in a checkerboard pattern. The coefficient matrix will vary between

$$A_1 = \begin{pmatrix} 2 & 1 \\ 1 & 4 \end{pmatrix} \quad A_2 = \begin{pmatrix} 4 & 2 \\ 2 & 8 \end{pmatrix} = 2A_1.$$

See Figure 4(a) for a surface plot of the resulting solution. Using the formula (3.3), we expect that the coefficient matrix should average to

$$\bar{A} = \begin{pmatrix} 8/3 & 4/3 \\ 4/3 & 16/3 \end{pmatrix}.$$

We set forcing  $f = 50$ , enforce zero Dirichlet boundary conditions, and run through different values of  $\epsilon$  to investigate the convergence of solutions of the original equation to solutions of the averaged equation as  $\epsilon \rightarrow 0$ .

Convergence results are presented in Table 1 and Figure 4(b). These computations are consistent with the assertion that the solutions of the original Equation (PDE) $^\epsilon$  do, in fact, converge to the solutions of the averaged Equation (2.3) as  $\epsilon \rightarrow 0$ . Furthermore, the convergence appears to be second order in  $\epsilon$ . That is, the exact solution of (PDE) $^\epsilon$  is given by

$$u^\epsilon = \bar{u} + O(\epsilon^2),$$

consistent with (2.4).

$\epsilon$	$\ u - \bar{u}\ _2$
1/3	$5.474 \times 10^{-3}$
1/5	$2.003 \times 10^{-3}$
1/7	$1.029 \times 10^{-3}$
1/9	$6.250 \times 10^{-4}$
1/11	$4.194 \times 10^{-4}$
1/13	$3.008 \times 10^{-4}$
1/15	$2.262 \times 10^{-4}$
1/17	$1.763 \times 10^{-4}$
1/19	$1.412 \times 10^{-4}$
1/21	$1.157 \times 10^{-4}$
1/23	$9.648 \times 10^{-5}$
1/25	$8.169 \times 10^{-5}$

TABLE 1. Results for a coefficient that is a multiple of a constant matrix. The error gives the  $L^2$  difference between the solution of the averaged equation and the solution of the original equation for a given value of  $\epsilon$ .

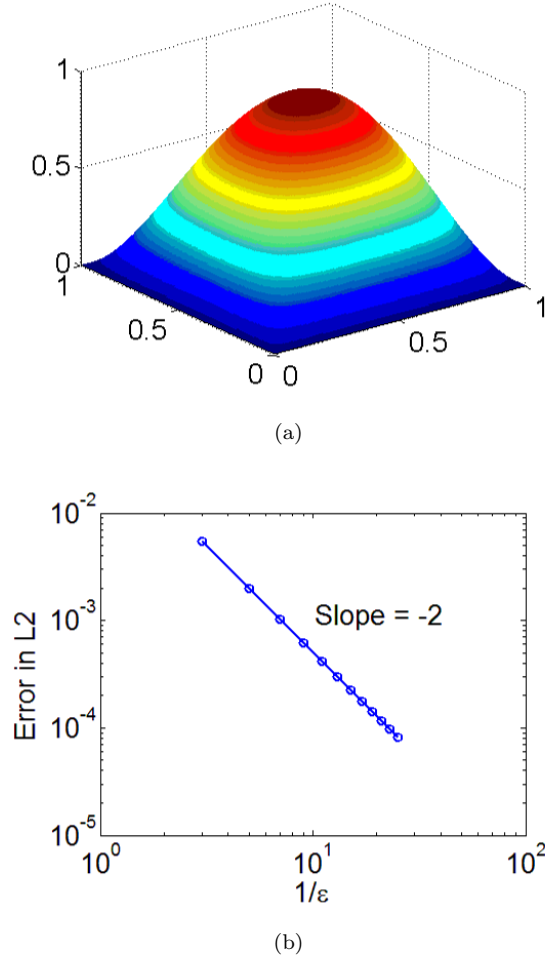


FIGURE 4. Results for a coefficient that is a multiple of a constant matrix. (a) A surface plot of the solution on the fully resolved grid ( $25 \times 25$  cells of  $24 \times 24$  grid points). (b) Log-log plot of  $L^2$  difference between solutions of averaged equation and original equation.

**5.3. A Layered Material.** Next we consider a layered material, where the coefficient matrix varies in vertical stripes. That is,  $A(y_1, y_2) = A(y_1)$ . For this example we allow the coefficients to vary between the following two matrices:

$$A_1 = \begin{pmatrix} 2 & 1 \\ 1 & 4 \end{pmatrix} \quad A_2 = \begin{pmatrix} 20 & 0 \\ 0 & 1 \end{pmatrix}.$$

Again we set the forcing to  $f = 50$  and enforce zero Dirichlet boundary conditions. The resulting solution is plotted in Figure 5.

According to (3.4) the homogenised coefficient matrix should be

$$\bar{A} = \begin{pmatrix} 40/11 & 10/11 \\ 10/11 & 41/11 \end{pmatrix}.$$

The difference between the solutions of the original equation (PDE) $^\epsilon$  and the homogenised equation (2.3) (measured in  $L^2$ ) are presented in Table 2 and Figure 5. As in the first example, we observe quadratic convergence as  $\epsilon \rightarrow 0$ .

$\epsilon$	$\ u - \bar{u}\ _2$
1/3	$1.565 \times 10^{-2}$
1/5	$5.609 \times 10^{-3}$
1/7	$2.867 \times 10^{-3}$
1/9	$1.740 \times 10^{-3}$
1/11	$1.168 \times 10^{-3}$
1/13	$8.384 \times 10^{-4}$
1/15	$6.312 \times 10^{-4}$
1/17	$4.924 \times 10^{-4}$
1/19	$3.948 \times 10^{-4}$
1/21	$3.237 \times 10^{-4}$
1/23	$2.702 \times 10^{-4}$
1/25	$2.289 \times 10^{-4}$

TABLE 2. Results for a layered material. The error gives the  $L^2$  difference between the solution of the averaged equation and the solution of the original equation for a given value of  $\epsilon$ .

**5.4. A Separable, Diagonal Coefficient Matrix.** Next we consider a separable, diagonal coefficient. We again choose a piecewise constant coefficient matrix. In this case, each cell is divided into quarters with the following coefficients:

$$\begin{aligned} A_1 &= \begin{pmatrix} 1 & 0 \\ 0 & 1 \end{pmatrix} \begin{pmatrix} 1 & 0 \\ 0 & 1 \end{pmatrix} & A_2 &= \begin{pmatrix} 2 & 0 \\ 0 & 4 \end{pmatrix} \begin{pmatrix} 1 & 0 \\ 0 & 1 \end{pmatrix} \\ A_3 &= \begin{pmatrix} 1 & 0 \\ 0 & 1 \end{pmatrix} \begin{pmatrix} 20 & 0 \\ 0 & 1 \end{pmatrix} & A_4 &= \begin{pmatrix} 2 & 0 \\ 0 & 4 \end{pmatrix} \begin{pmatrix} 20 & 0 \\ 0 & 1 \end{pmatrix}. \end{aligned}$$

As before we set  $f = 50$  with  $u = 0$  on the boundary. See Figure 6(a) for a surface plot of the solution.

According to (3.5), the homogenised coefficients should be

$$\bar{A} = \begin{pmatrix} 14 & 0 \\ 0 & 2 \end{pmatrix}.$$

As in the previous examples, we observe  $O(\epsilon^2)$  convergence to the solution of the averaged equation; see Table 3 and Figure 6(b).

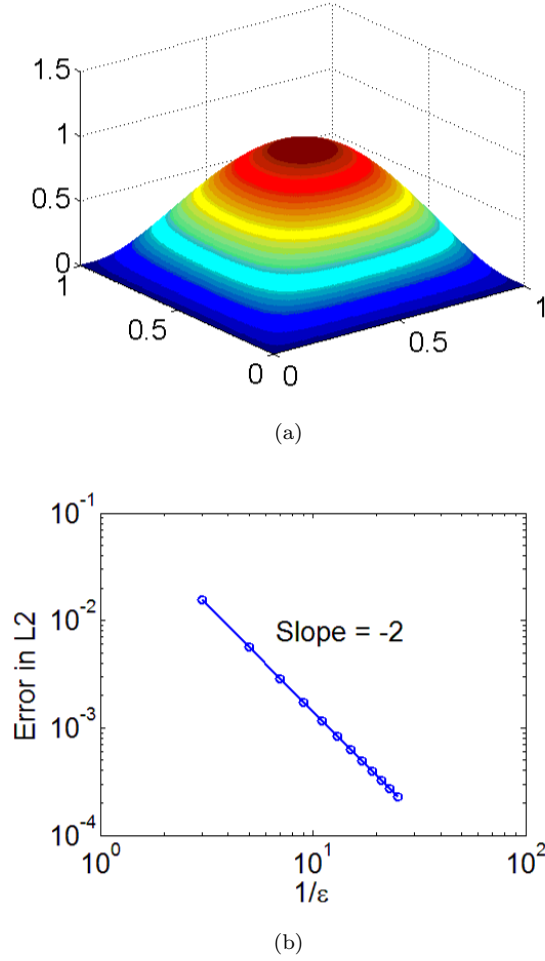


FIGURE 5. Results for a layered material. (a) A surface plot of the solution on the fully resolved grid ( $25 \times 25$  cells of  $24 \times 24$  grid points). (b) Log-log plot of  $L^2$  difference between solutions of the averaged equation and original equation.

**5.5. A More General Linear Operator.** In all the examples we have considered so far we have assumed that the coefficients of the drift and source terms ( $b, c$  in (1.1)) are equal to zero. Here we consider a more general operator where these terms are present in the equation. We choose the same coefficient matrix used in Section 5.2, which is a scalar multiple of a constant matrix. The remaining coefficients do not need to have this property (i.e.,  $b$  need not be a multiple of a constant vector) in order for the analysis in Section 3.1 to apply. In particular we

$\epsilon$	$\ u - \bar{u}\ _2$
1/3	$6.105 \times 10^{-2}$
1/5	$2.337 \times 10^{-2}$
1/7	$1.214 \times 10^{-2}$
1/9	$7.405 \times 10^{-3}$
1/11	$4.984 \times 10^{-3}$
1/13	$3.582 \times 10^{-3}$
1/15	$2.698 \times 10^{-3}$
1/17	$2.106 \times 10^{-3}$
1/19	$1.689 \times 10^{-3}$
1/21	$1.385 \times 10^{-3}$
1/23	$1.156 \times 10^{-3}$
1/25	$9.794 \times 10^{-4}$

TABLE 3. Results for a coefficient matrix with separable entries. The error gives the  $L^2$  difference between the solution of the averaged equation and the solution of the original equation for a given value of  $\epsilon$ .

consider the coefficients:

$$A_1 = \begin{pmatrix} 2 & 1 \\ 1 & 4 \end{pmatrix} \quad b_1 = \begin{pmatrix} 1 \\ 1 \end{pmatrix} \quad c_1 = 1$$

$$A_2 = \begin{pmatrix} 4 & 2 \\ 2 & 8 \end{pmatrix} \quad b_2 = \begin{pmatrix} 2 \\ 4 \end{pmatrix} \quad c_1 = 2.$$

As before we let  $f = 50$  and enforce zero Dirichlet boundary conditions. The solution is plotted in Figure 7(a).

The analysis in Section 3.1 is easily extended to this situation, and predicts the following averaged coefficients:

$$\bar{A}_1 = \begin{pmatrix} 8/3 & 4/3 \\ 4/3 & 16/3 \end{pmatrix} \quad \bar{b}_1 = \begin{pmatrix} 4/3 \\ 2 \end{pmatrix} \quad \bar{c}_1 = 4/3.$$

Convergence results are contained in Table 4 and Figure 7. As before, we observe quadratic convergence as  $\epsilon \rightarrow 0$ .

**5.6. Non-Zero Boundary Conditions.** In all the examples we have studied so far we have enforced zero Dirichlet boundary conditions. Now we demonstrate numerically that the approach presented in this paper also works for non-constant Dirichlet boundary conditions.

In this example we use the  $y$ -periodic coefficient matrix with entries

$$a_{11}^\epsilon = \frac{1}{\cos\left(\frac{2\pi x_1}{\epsilon} - \frac{\pi}{\epsilon}\right) \left[\cos\left(\frac{\pi}{\epsilon}\right) - \cos\left(\frac{2\pi x_2}{\epsilon} - \frac{\pi}{\epsilon}\right)\right] + 4}$$

$$a_{22}^\epsilon = \frac{1}{\cos\left(\frac{2\pi x_2}{\epsilon} - \frac{\pi}{\epsilon}\right) \left[\cos\left(\frac{\pi}{\epsilon}\right) - \cos\left(\frac{2\pi x_1}{\epsilon} - \frac{\pi}{\epsilon}\right)\right] + 4}$$

$$a_{12} = 0.$$

We set forcing

$$f = -2$$

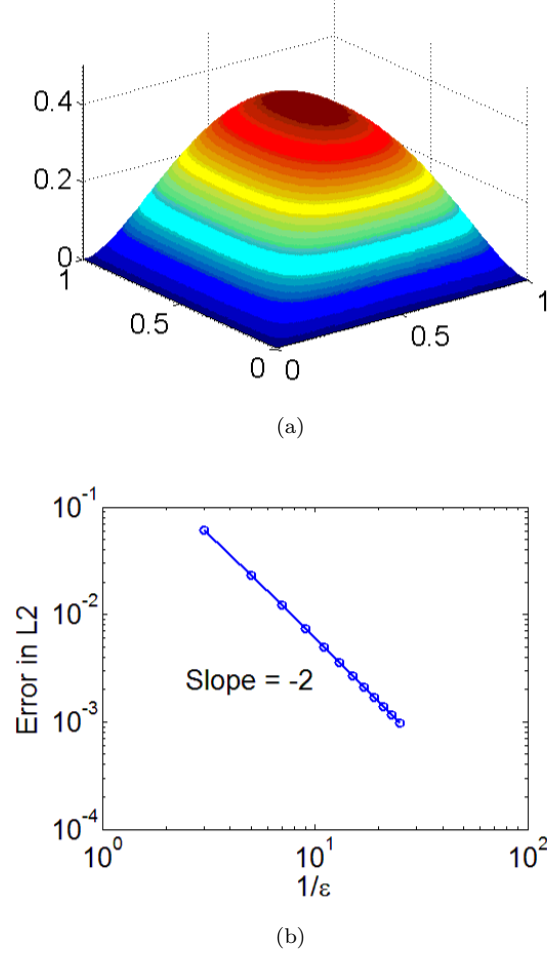


FIGURE 6. Results for a coefficient matrix with separable entries. (a) A surface plot of the solution on the fully resolved grid ( $25 \times 25$  cells of  $24 \times 24$  grid points). (b) Log-log plot of  $L^2$  difference between solutions of the averaged equation and original equation.

and enforce the boundary conditions

$$u = 2x_1^2 + 2x_2^2 \quad x_1 = 0, x_1 = 1, x_2 = 0, x_2 = 1.$$

This problem has the exact solution

$$u^\epsilon = \frac{\epsilon^2}{4\pi^2} \left[ \cos\left(\frac{\pi}{\epsilon}\right) - \cos\left(\frac{2\pi x_1}{\epsilon} - \frac{\pi}{\epsilon}\right) \right] \left[ \cos\left(\frac{\pi}{\epsilon}\right) - \cos\left(\frac{2\pi x_2}{\epsilon} - \frac{\pi}{\epsilon}\right) \right] + 2x_1^2 + 2x_2^2.$$

We fix  $\epsilon = 1/499$  and look at the relationship between cell resolution and solution accuracy. This solution is plotted in Figure 8(a).

$\epsilon$	$\ u - \bar{u}\ _2$
1/3	$5.486 \times 10^{-3}$
1/5	$2.008 \times 10^{-3}$
1/7	$1.031 \times 10^{-3}$
1/9	$6.263 \times 10^{-4}$
1/11	$4.203 \times 10^{-4}$
1/13	$3.014 \times 10^{-4}$
1/15	$2.267 \times 10^{-4}$
1/17	$1.767 \times 10^{-4}$
1/19	$1.415 \times 10^{-4}$
1/21	$1.159 \times 10^{-4}$
1/23	$9.669 \times 10^{-5}$
1/25	$8.187 \times 10^{-5}$

TABLE 4. Results for a general elliptic operator. The error gives the  $L^2$  difference between the solution of the averaged equation and the solution of the original equation for a given value of  $\epsilon$ .

The convergence results are presented in Table 5 and Figure 8(b). It is evident from the log-log plot of error that for fixed (small)  $\epsilon$ , the error is linearly dependent on the spatial step size used to solve the cell problem (2.1).

$1/h$	$\bar{a}_{11}$	$\bar{a}_{22}$	$\ u - \bar{u}\ _2$
10	0.24514	0.24514	$6.527 \times 10^{-3}$
50	0.24891	0.24891	$1.437 \times 10^{-3}$
90	0.24939	0.24939	$8.103 \times 10^{-4}$
130	0.24958	0.24958	$5.607 \times 10^{-4}$
170	0.24967	0.24967	$4.290 \times 10^{-4}$
210	0.24973	0.24973	$3.499 \times 10^{-4}$
250	0.24978	0.24978	$2.907 \times 10^{-4}$
290	0.24981	0.24981	$2.531 \times 10^{-4}$
330	0.24983	0.24983	$2.239 \times 10^{-4}$
370	0.24985	0.24985	$1.989 \times 10^{-4}$
410	0.24986	0.24986	$1.792 \times 10^{-4}$
450	0.24988	0.24988	$1.630 \times 10^{-4}$
490	0.24989	0.24989	$1.494 \times 10^{-4}$

TABLE 5. Results for a problem with non-constant boundary conditions homogenised on a cell with spatial resolution  $h$ . The averaged coefficients are  $\bar{a}_{11}, \bar{a}_{22}, \bar{a}_{12}$ . The error gives the  $L^2$  difference between the solution of the homogenised equation and the solution of the original equation.

**5.7. Random Coefficients.** So far we have considered operators that vary periodically. However, the averaging method discussed in this article can also be applied to average random operators. While we avoid the analysis, we can compute the invariant distribution in this case.

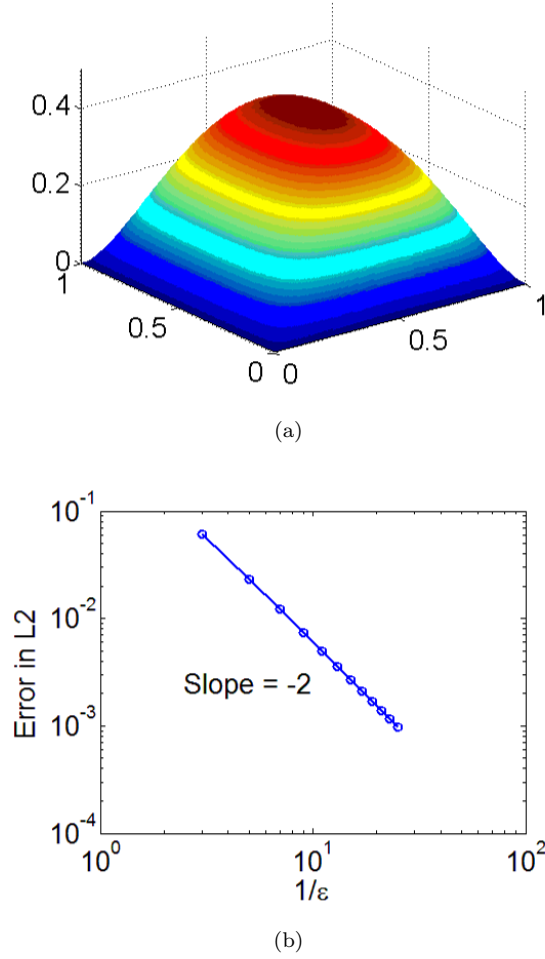


FIGURE 7. Results for a general elliptic operator. (a) A surface plot of the solution on the fully resolved grid ( $25 \times 25$  cells of  $24 \times 24$  grid points). (b) Log-log plot of  $L^2$  difference between solutions of the averaged equation and original equation.

Next we consider the case where the coefficient matrix at each point is randomly chosen (with equal probability) to be one of two constant operators. Since the operator no longer varies periodically, it is now necessary to solve for the invariant distribution in the entire domain. As before, we enforce periodic boundary conditions. In order to compute the averaged coefficients, we solve for the invariant distribution with  $K$  different randomly chosen coefficients  $A^i$  and compute the averaged coefficients

$$\bar{A}^i = \langle \rho^\infty A^i \rangle.$$

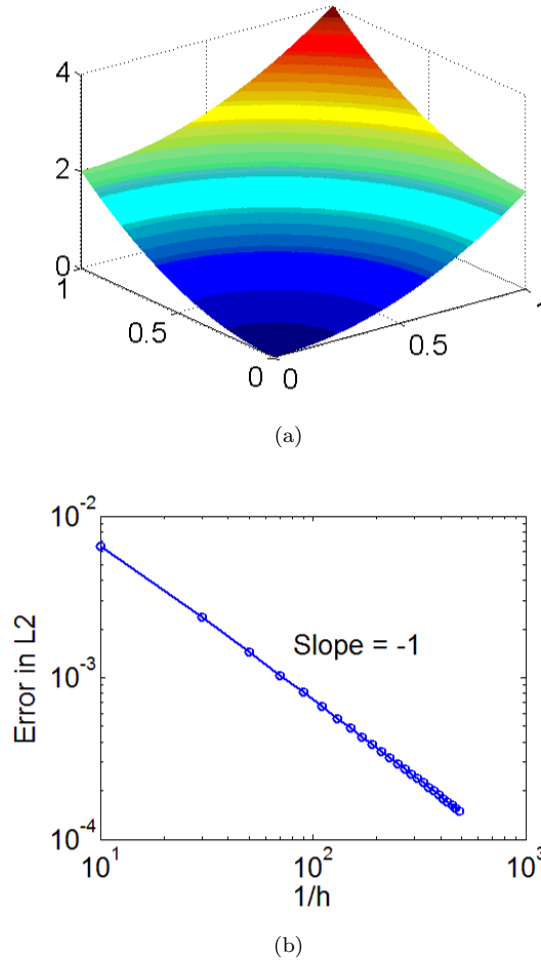


FIGURE 8. Results for a problem with non-constant boundary data averaged on a cell with spatial resolution  $h$ . (a) A surface plot of the exact solution (with  $\epsilon = 1/499$ ). (b) Log-log plot of  $L^2$  difference between solutions of the averaged equation and original equation.

The results of these trials are averaged to compute the averaged coefficient matrix for the general random problem.

$$\bar{A} = \frac{1}{K} \sum_{i=1}^K \bar{A}^i.$$

In the following computations, we average the coefficients over  $K = 10$  trials. To demonstrate that this approach correctly averages the random operator we will solve for twenty different random coefficient matrices and compute the mean difference between the solutions of the random and averaged problems.

In particular, we randomly vary between the following two coefficient matrices:

$$A_1 = \begin{pmatrix} 2 & 1 \\ 1 & 4 \end{pmatrix} \quad A_2 = \begin{pmatrix} 20 & 0 \\ 0 & 1 \end{pmatrix}.$$

We enforce zero Dirichlet boundary conditions and set forcing  $f = 30$ .

Results are shown in Table 6 and Figure 9. We see that as the number of grid points is increased, the solution of the random equation approaches (on average) the solution of the averaged equation. Moreover, the average difference between the two solutions is  $O(h)$ .

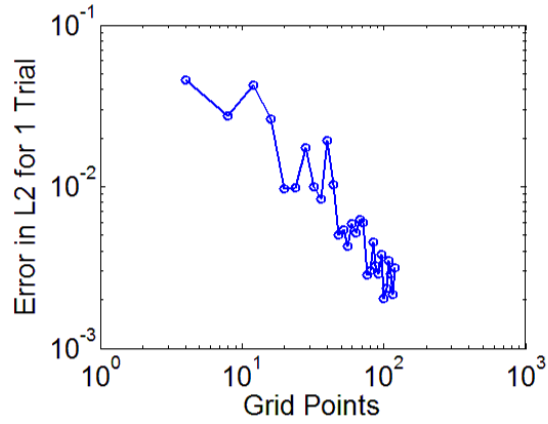
$N$	$\bar{a}_{11}$	$\bar{a}_{22}$	$\bar{a}_{12}$	$\ u - \bar{u}\ _2$	$\langle \ u - \bar{u}\ _2 \rangle$
8	6.834	3.194	0.731	$2.747 \times 10^{-2}$	$3.635 \times 10^{-2}$
16	6.745	3.209	0.736	$2.622 \times 10^{-2}$	$2.146 \times 10^{-2}$
24	6.657	3.224	0.741	$9.839 \times 10^{-3}$	$1.699 \times 10^{-2}$
32	6.628	3.229	0.743	$9.934 \times 10^{-3}$	$9.940 \times 10^{-3}$
40	6.672	3.221	0.740	$1.923 \times 10^{-2}$	$8.358 \times 10^{-3}$
48	6.683	3.220	0.740	$5.064 \times 10^{-3}$	$6.583 \times 10^{-3}$
56	6.538	3.244	0.748	$4.283 \times 10^{-3}$	$6.029 \times 10^{-3}$
64	6.496	3.251	0.750	$5.144 \times 10^{-3}$	$6.624 \times 10^{-3}$
72	6.624	3.229	0.743	$5.976 \times 10^{-3}$	$5.100 \times 10^{-3}$
80	6.636	3.227	0.742	$3.008 \times 10^{-3}$	$4.009 \times 10^{-3}$
88	6.594	3.234	0.745	$3.239 \times 10^{-3}$	$3.454 \times 10^{-3}$
96	6.592	3.235	0.745	$3.821 \times 10^{-3}$	$3.902 \times 10^{-3}$
104	6.564	3.239	0.746	$2.369 \times 10^{-3}$	$3.145 \times 10^{-3}$
112	6.574	3.238	0.746	$2.870 \times 10^{-3}$	$2.979 \times 10^{-3}$
120	6.572	3.238	0.746	$3.141 \times 10^{-3}$	$2.986 \times 10^{-3}$

TABLE 6. Results for a problem with random coefficients on an  $N \times N$  grid. The averaged coefficients are  $\bar{a}_{11}, \bar{a}_{22}, \bar{a}_{12}$ . The errors include the  $L^2$  difference between the solution of the homogenised equation and the solution of a random equation as well as the average difference over 20 trials.

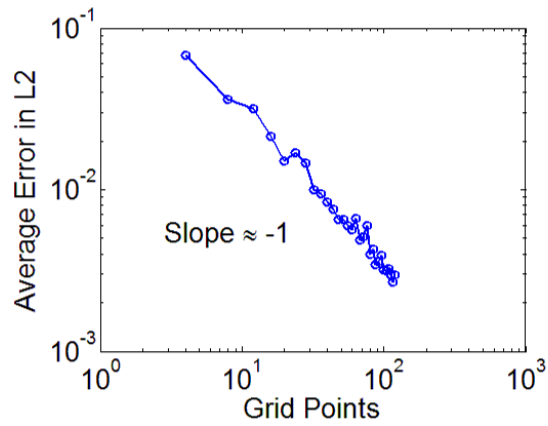
## 6. CONCLUSIONS

We recovered a simple formula for the averaged operator of the non-divergence structure elliptic operator with rapidly varying, periodic coefficients. This formula was available in the literature using probabilistic techniques; we gave a formal derivation using Partial Differential Equations techniques. The derivation can be made rigorous. We also presented several special cases where the adjoint problem could be solved in closed form, leading to a closed form result for the averaged operator. This could be accomplished for a wider set of examples than in the divergence structure case. We also showed that the homogenised operators are generally different between the two cases.

The second part was numerical computations. The adjoint equation was discretised using finite differences, and solved using a Gauss-Seidel method. The effort involved in solving this problem is comparable (or less) that the corresponding



(a)



(b)

FIGURE 9. Results for a problem with random coefficients. (a) Log-log plot of the  $L^2$  difference between the homogenised solution and a random solution. (b) Log-log plot of the average  $L^2$  difference between the homogenised solution and a random solution over 20 trials.

problem in the divergence structure case. The numerics were validated for finite  $\epsilon$  against resolved numerical solutions. The formal asymptotic convergence rate  $O(\epsilon^2)$  was also validated.

#### REFERENCES

- [1] Doina Cioranescu and Patrizia Donato. *An introduction to homogenization*, volume 17 of *Oxford Lecture Series in Mathematics and its Applications*. The Clarendon Press Oxford University Press, New York, 1999.
- [2] B. Engquist and P. E. Souganidis. Asymptotic and numerical homogenization. *Acta Numer.*, 17:147–190, 2008.

- [3] M. I. Freidlin. Dirichlet's problem for an equation with periodic coefficients depending on a small parameter. *Theory Prob. Appl.*, 9:121–125, 1964.
- [4] Mark H. Holmes. *Introduction to perturbation methods*, volume 20 of *Texts in Applied Mathematics*. Springer-Verlag, New York, 1995.
- [5] Harold J. Kushner and Paul Dupuis. *Numerical methods for stochastic control problems in continuous time*, volume 24 of *Applications of Mathematics (New York)*. Springer-Verlag, New York, second edition, 2001. Stochastic Modelling and Applied Probability.
- [6] Graeme W. Milton. *The theory of composites*, volume 6 of *Cambridge Monographs on Applied and Computational Mathematics*. Cambridge University Press, Cambridge, 2002.
- [7] Houman Owhadi and Lei Zhang. Homogenization of parabolic equations with a continuum of space and time scales. *SIAM J. Numer. Anal.*, 46(1):1–36, 2007/08.
- [8] Grigorios A. Pavliotis and Andrew M. Stuart. *Multiscale methods*, volume 53 of *Texts in Applied Mathematics*. Springer, New York, 2008. Averaging and homogenization.
- [9] Hongyun Wang. Convergence of a numerical method for solving discontinuous Fokker-Planck equations. *SIAM J. Numer. Anal.*, 45(4):1425–1452 (electronic), 2007.
- [10] Hongyun Wang, Charles S. Peskin, and Timothy C. Elston. A robust numerical algorithm for studying biomolecular transport processes. *J. Theoret. Biol.*, 221(4):491–511, 2003.